Title	Coating of High Corrosion Resistant Amorphous Stainless Steels by RF Sputtering(Materials, Metallurgy & Weldability)
Author(s)	Naka, Masaaki; Matsumoto, Yoshinori
Citation	Transactions of JWRI. 1993, 22(1), p. 55-60
Version Type	VoR
URL	https://doi.org/10.18910/7927
rights	
Note	

Coating of High Corrosion Resistant Amorphous Stainless Steels by RF Sputtering†

Masaaki NAKA* and Yoshinori MATSUMOTO**

Abstract

Corrosion resistant amorphous $(SUS316)_{100-x}Zr_x$ stainless steels were prepared by R.F. magnetron sputtering in argon gas. The alloying of zirconium effectively stabilizes the amorphous structure in zirconium content from 3.2 at% to 47.7 at%. The corrosion resistance of (SUS316) stainless steel in 1N HCl was definitely improved by amorphization. Although the high corrosion resistance is realized against the smooth and flat surface of the amorphous stainless alloys, an increase in surface roughness degrades the corrosion resistance. The $(SUS316)_{100-x}Zr_x$ amorphous stainless steels with high microhardness represent the high maximum value at zirconium content of 30 at%, suggesting the local bonding of zirconium and iron.

KEY WORDS:(Stainless Steel)(Amorphous Alloy)(Corrosion)(Corrosion Resistance)(Coating)(Sputtering)

1. Introduction

Amorphous alloys have received considerable interest with regard to their corrosion properties. The beneficial properties of amorphous alloys is the chemical homogeneity that has no crystalline defects such as grain boundaries and precipitous.

Metalloids affect the corrosion behavior of amorphous alloys. Phosphorus among metalloids assists in forming the superior protective film in chromium-containing amorphous alloys [1, 2]. On the other hand, the admixture of chromium and molybdenum definitely improves the corrosion resistance of zirconium -containing amorphous alloys without metalloids [3-6].

The quenching rate for the formation of amorphous alloys from the liquid state restricts the shape of the alloys. This paper describes the attempt to form corrosion-resistant amorphous FeNiCrMoZr alloy film on various substrates the physical and chemical properties of the films.

2. Experimental Procedures

The targets used in 100 mm diameter and 4 mm thickness composed of SUS316 (which corresponds to AISI316) and pure zirconium plates. High sputtering rates were maintained by R.F. magnetron type sputtering in 6.65 MPa argon gas. The substrates of copper, iron and SUS304 stainless steel were water-cooled. The sputtering power and time of 400 W and 7.2 ks, and the film thickness of alloys were 15 μm. The chemical compositions of the sputtered alloys are listed in **Table 1**. The surface roughness of copper substrates was changed by polishing with SiC paper or buff cloth or argon-sputtering. The structure of sputtered films was investigated by X-ray diffractometry with Cu K . The corrosion resistance of the film was determined by the

Table 1 Chemical compositions of SUS316 and sputtered alloys.

No.	Composition (at%)				
	Zr	Fe	Ni	Cr	Mo
1	0.00	65.70	11.49	18.88	1.21
2	0.00	67.63	11.43	17.14	1.38
3	2.16	65.05	12.12	18.52	0.95
4	3.23	65.25	11.76	17.95	0.93
5	6.94	63.49	10.49	18.29	0.80
6	7.48	62.26	11.35	17.06	0.92
7	8.45	62.37	10.41	17.96	0.81
8	13.51	57.55	10.75	15.78	0.82
9	13.94	57.31	10.52	15.79	0.79
10	14.40	57.10	10.73	15.86	0.84
11	17.60	54.95	10.12	15.49	0.88
12	18.09	54.53	10.17	14.85	0.83
13	22.63	51.43	9.06	15.20	0.89
14	26.88	49.11	9.08	13.36	0.83
15	35.32	43.43	8.09	11.84	0.65
16	42.37	38.83	7.18	10.48	0.56
17	47.69	35.84	6.10	9.97	0.41

† Received on July 30, 1993

* Professor
** Graduate Student

Transactions of JWRI is published by Welding Research Institute, Osaka University, Ibaraki, Osaka 567, Japan

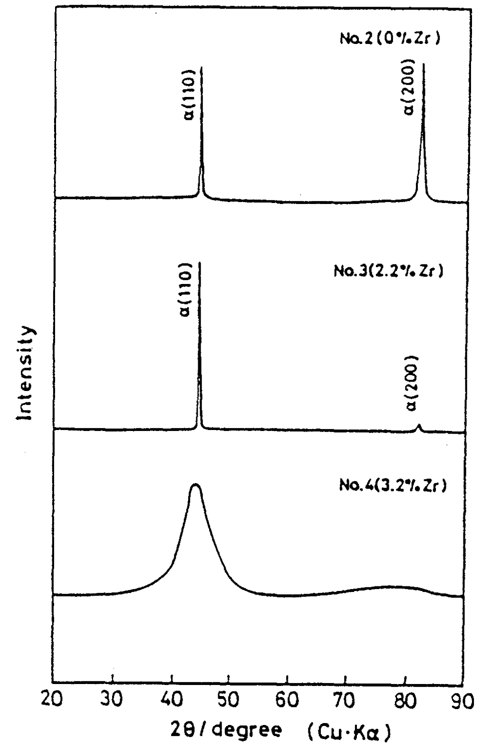

Fig. 1a X-ray diffraction patterns of sputtered alloys.

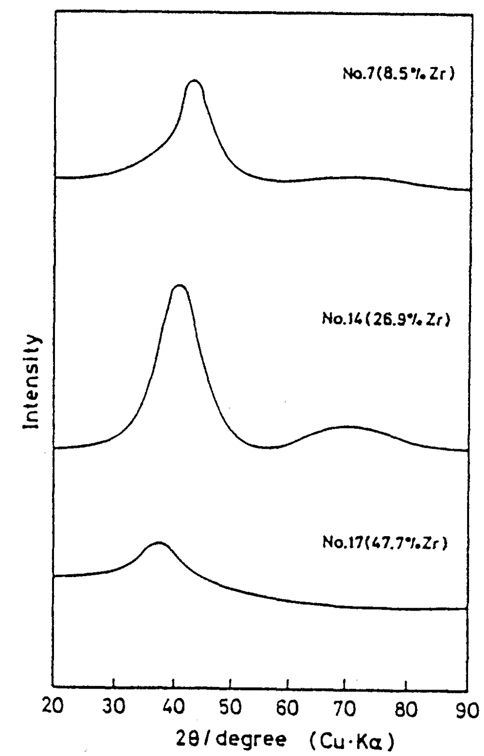

Fig. 1b X-ray diffraction patterns of sputtered alloys.

potentiodynamic method with a potential sweep rate of 2.5×10^{-3} Vs^{-1} in 1N HCl. The microhardness of the films was measured with 25 g load.

3. Results and Discussion

Figures 1 a and b show the X-ray diffraction patterns of sputtered $(SUS316)_{100-x}Zr_x$ alloys. The structure of SUS316(no.2) and 2.16 at% Zr(no.3) alloys sputtered are b.c.c. phase which are different from f.c.c. phase of the SUS316 target. The structure of the sputtered alloys containing Zr content from 3.2 at% up to 47.7 at%Zr becomes amorphous. Their X-ray diffraction patterns present only a few diffuse peaks. The angle of first peak in the diffraction patterns shifts to the lower with increasing Zr content.

The mixing of zirconium with alloys definitely stabilizes the amorphous structure. **Fig. 2** shows the compositional range for glass formation of some amorphous alloys. The glass formation range of $(SUS316)_{100-x}Zr_x$ alloys expands to the lower alloying content side than that of sputtered $Fe_{100-x}Zr_x$ [7], $(AISI304)_{100-x}W_x$(x=11-54) [8] and $Fe_{100-x}Ti_x$ (x=20-75) [9] alloy.

The amorphous $(SUS316)_{100-x}Zr_x$ alloys were also covered on various water-cooled substrates of copper(a), iron(b) and stainless steel(c) as shown in **Fig. 3.** The energy of argon ions in plasma transfers to the atoms of substrates in the system, and the sputtered atoms deposit on substrates. The energies of atoms sputtered is higher than that of simply vaporized atoms. In other

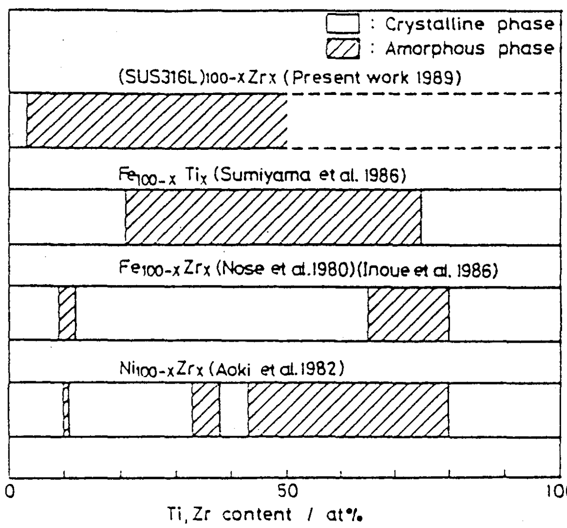

Fig. 2 Glass formation range of amorphous alloys.

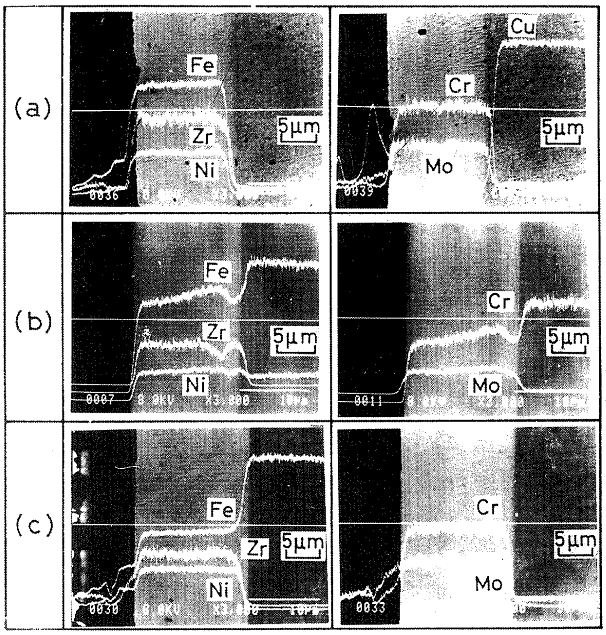

Fig. 3 Line analyses of cross section of sputtered amorphous $(SUS316)_{100-x}Zr_x$(x=14.4, no.14) alloy.

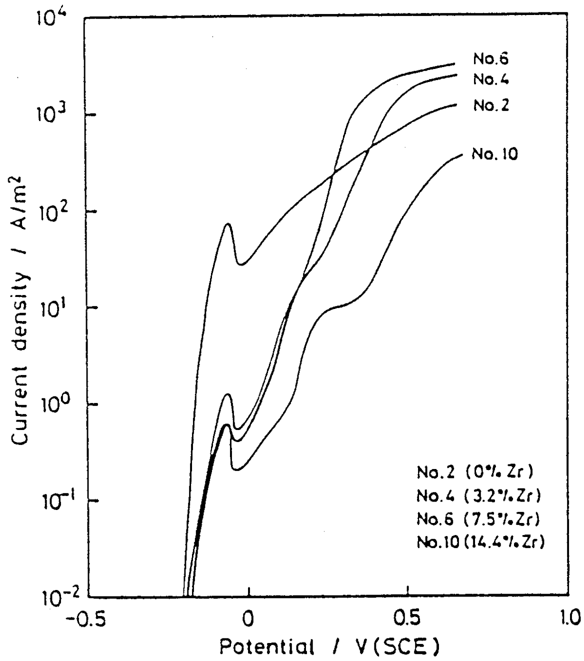

Fig. 4 Anodic polarizarion curves of sputtered crystalline SUS316 stainless steel and sputtered amorphous $(SUS316)_{100-x}Zr_x$ alloys in 1N HCl.

words, the sputtering technique makes the coating of the film on a variety of substrates.

The corrosion properties of sputtered films are evaluated by measuring the polarization curves in 1N HCl. The anodic polarization curves of crystalline SUS316 target and the sputtered alloys and amorphous $(SUS316)_{100-x}Zr_x$ alloys in 1N HCl are shown in 1N HCl are shown in **Figs. 4** and **5**. The sputtering conditions of the alloys were 400 W, 6.65 Pa and 7.2 ks, where the substrates were sputtered under the conditions of 50 W, 6.65 Pa and 0.3 ks. Although the corrosion potential of SUS316 (no. 1) alloy shifts to the noble side by sputtering (no. 1) alloy to (no. 2) alloy, the passivation current density of sputtered SUS316 (no. 2) alloy is higher than that of (SUS316) (no. 1) alloy. This means that the corrosion resistance of stainless steel is not improved by changing to the microcrystalline structure owing to sputtering. On the other hand, the glass formation of $(SUS316)_{100-x}Zr_x$ alloy with the addition of zirconium ennobles the corrosion potential to the noble side and reduces the passivation current density as shown in **Figs. 6** and **7**, where the corrosion potentials and the passivation current densities of amorphous alloys are plotted against Zr content in the alloys, respectively. The passivation current densities of amorphous alloys are one or two orders of magnitude lower than that of crystalline SUS316 and sputtered SUS316 alloys.

In the acid solution containing chlorine ions the conventional stainless steels suffer from pitting corrosion. The amorphous alloys, however, possess no crystalline defects such as grain boundaries and precipitates of carbides, and are chemically homogeneous. This compositional homogeneity of amorphous alloys is attributable to the high corrosion resistance against local pitting corrosion of chlorine ions.

The increase in zirconium content in amorphous alloys does not effectively reduce the passivation current densities. This implies that zirconium is not the main element for the protective film of alloys. The protective film is composed of oxyhydroxide of chromium [3].

The surface structure of amorphous 14.4 at%Zr (no. 10) with the surface treatment of substrate is shown in **Fig. 8**, where the substrates are treated with buff cloth polishing (A), buff cloth polishing+sputtering etching (50 W, 0.3ks) (B), buch cloth polishing+sputtering etching (100W, 0.9ks) (C), and SiC paper (#1000) polishing (D). The roughness of the surface of the amorphous alloys rises in the sequence of A, B, C and D. In D, some small cracks along the polishing traces are seen. The change in anodic polarization curves of amorphous 14.4 at% Zr (no. 10) alloy with surface

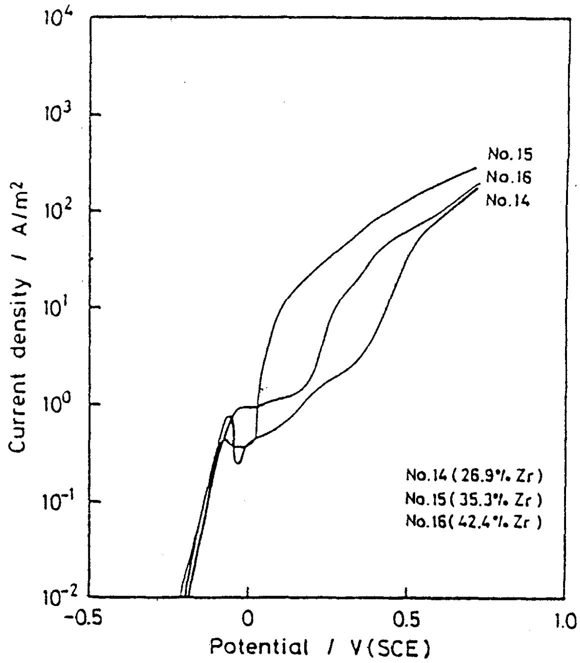

Fig. 5 Anodic polarization curves of sputtered crystalline (SUS316) stainless steel and sputtered amorphous $(SUS316)_{100-x}Zr_x$ alloys in 1N HCl.

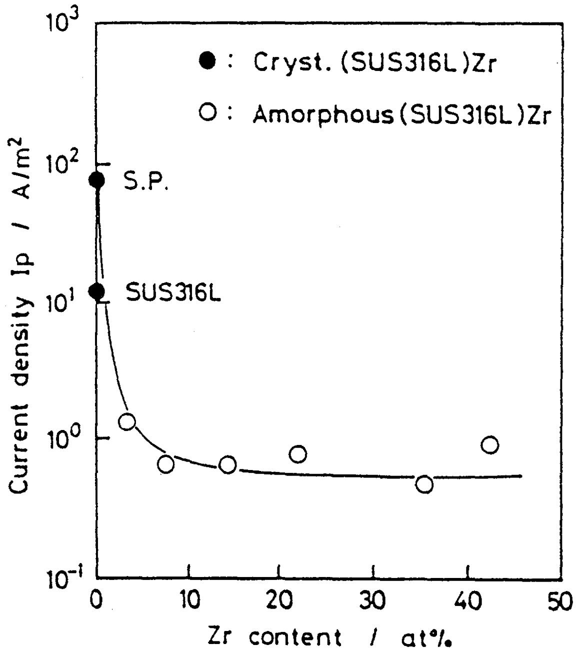

Fig. 7 Compositional dependence of passivation current densities for sputtered $(SUS316)_{100-x}Zr_x$ alloys.

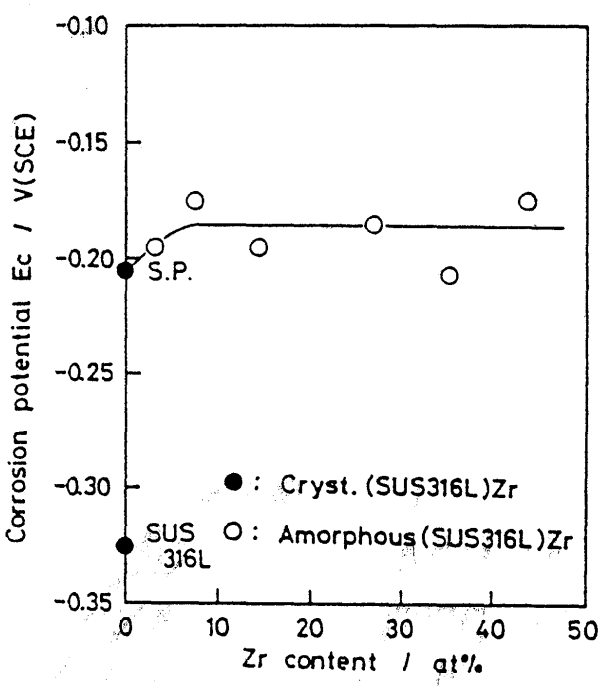

Fig. 6 Compositional dependence of corrosion potentials of sputtered $(SUS316)_{100-x}Zr_x$ alloys.

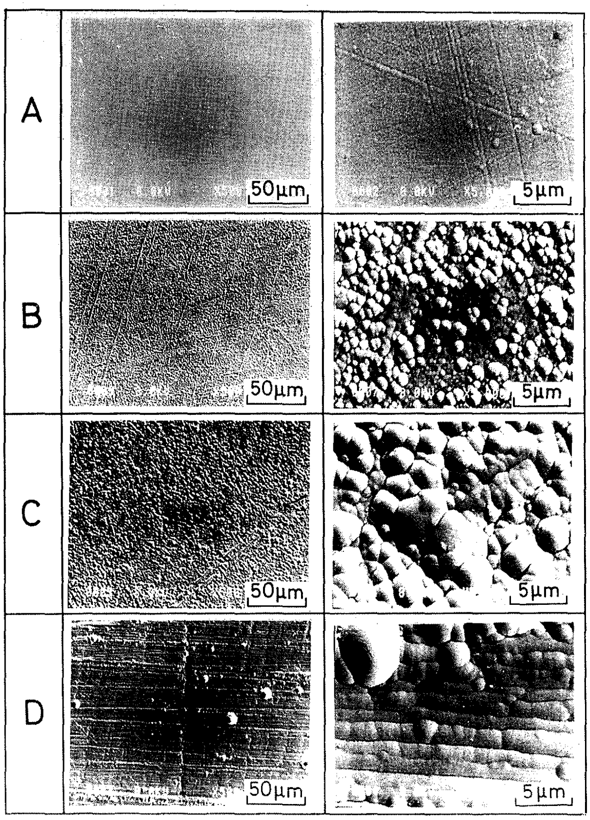

Fig. 8 Surface structure of sputtered amorphous $(SUS316)_{85.6}Zr_{14.4}$(no. 10) alloys.

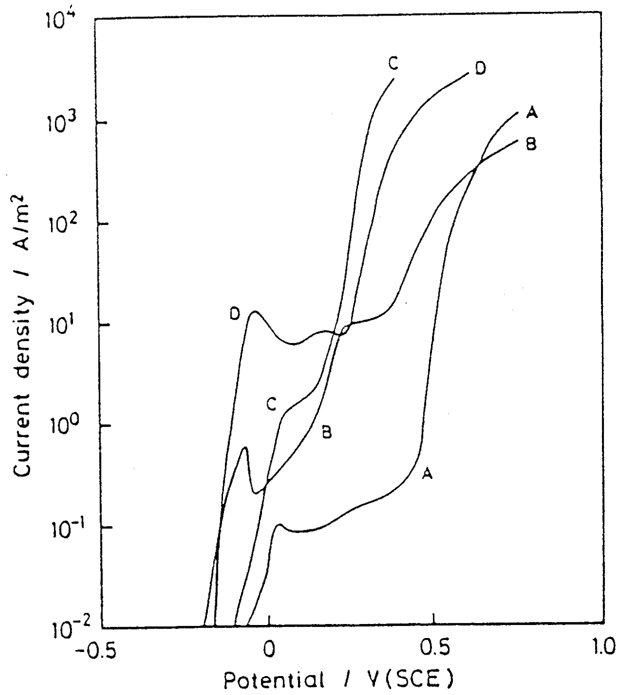

Fig. 9 Change in anodic polarization curves of sputtered alloys with the surface roughness.

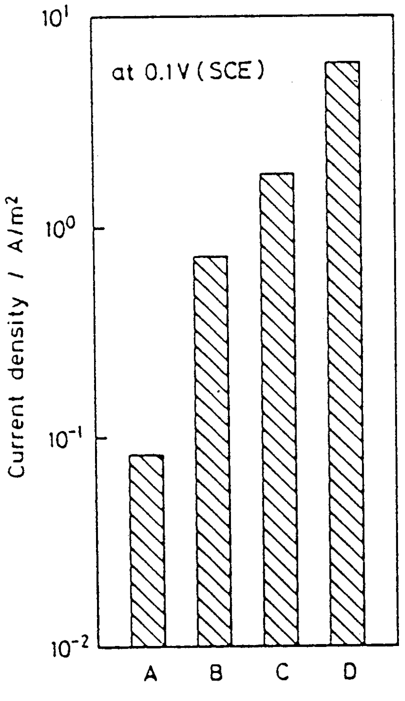

Fig. 10 Change in current densities at 0.1 V(SCE) of amorphous $(SUS316)_{85.6}Zr_{14.4}$ alloy with surface roughness.

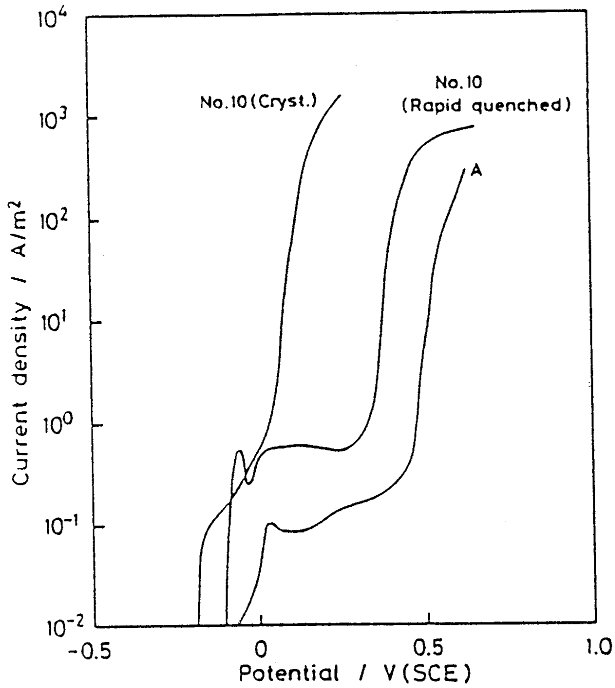

Fig. 11 Anodic polarization curves of amorphous and crystalline $(SUS316)_{85.6}Zr_{14.4}$ alloys.

in argroughness is shown in **Fig. 9**, where the curve B corresponds to that of no. 10 alloy in Fig. 2. The current densities of amorphous alloys at the passivate current densities at 0.1 V(SCE) increase with an increase in surface roughness as shown in **Fig. 10.** This indicates that the corrosion resistance of the amorphous alloys changes with the surface roughness, although the amorphization of stainless steel improves the corrosion resistance. The convex parts in the surface of alloys operates as active corrosion points in amorphous alloys without crystalline defects. The corrosion resistance of amorphous FeNiCrMoZr alloys degrades as the active points on the alloy surface increase, though the smooth alloys exhibit high corrosion resistance.

In other words, the high corrosion resistance of amorphous FeNiCrMoZr alloys is realized in the smooth flat surface without the chemically active points against corrosion.

The sputtering amorphous $(SUS316)_{100-x}Zr_x$ alloy with x=14.4 represents the higher corrosion resistance than that of crystalline alloy and also that of liquid-quenched alloy which possesses the same composition as shown in **Fig. 11.** This result indicates that the smooth surface of amorphous alloys can be realized if the surface of substrate is properly prepared.

The micro hardness of amorphous $(SUS316)_{100-x}Zr_x$ alloys are shown in **Fig. 12,** including the values of amorphous FeZr alloys [9] and NiZr alloys [10]. The microhardness of amorphous $(SUS316)_{100-x}Zr_x$ alloys relatively higher than that of SUS316 and copper, and around the zirconium content of 30 at%, which

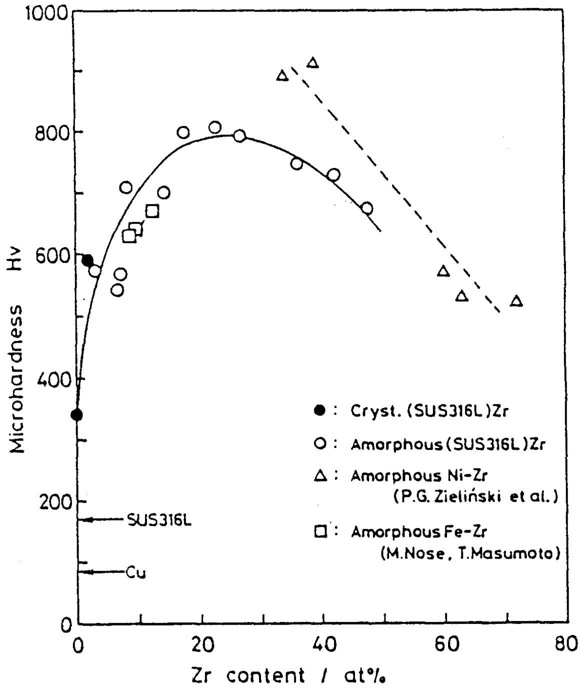

Fig. 12 Compositional dependence of microhardness of sputtered $(SUS316)_{100-x}Zr_x$ alloys.

composition corresponds to the zirconium content of $ZrFe_2$ compounds. This suggests that the local bonding of iron and zirconium is formed in the amorphous alloys.

4. Conclusions

The amorphous $(SUS316)_{100-x}Zr_x$ alloys were formed by sputtering SUS316 steels and zirconium plateson gas. The corrosion behavior of sputtered alloys was investigated by a potentiodynamic method in 1N HCl. The zirconium stabilizes the amorphous structure at zirconium content from 3.2 to 47.7 at%. Although the SUS316 f.c.c. stainless steel with zirconium content below 2.16 at% transforms to b.c.c. crystalline stainless steel on sputtering, the corrosion resistance of the alloy is not effectively improved.

On the other hand, the sputtered $(SUS316)_{100-x}Zr_x$ exhibits a superior corrosion resistance by amorphizing at zirconium content from x=3.2 to 47.7. The corrosion potentials move to the noble side and the passivation current densities definitely decrease on amorphization.
The corrosion resistance of amorphous alloys degrades with the surface roughness. The superior corrosion resistance of the amorphous alloys is realized against the smooth and flat surface of the alloys. The sputtered amorphous stainless steels show a high microhardness around the zirconium content of 30 at%, suggesting the local bonding of iron and zirconium in the alloys.

References

1) M. Naka, K. and T. Masumoto, J. Japan Inst. Met., 38(1976)385.
2) K. Hashimoto, M. Naka, K. Asami and T. Mastumoto, Corrosion Eng., 27(1978)279.
3) M. Naka, M. Miyake and I. Okamoto, Scr. Metall, 17(1983)1293.
4) M. Naka, M. Miyake and I. Okamoto, J. Non-cryst. Solids, 95&96(1987)1071.
5) M. Naka, M. Miyake and I. Okamoto, Trans. Japan Inst. Met. Suppl., 22(1988)447.
6) M. Naka, M. Miyake and I. Okamoto, J. Non-cryst. Solids, 117&118(1990)658.
7) R. Wang, J. Mater. Sci., 17(1982)1142.
8) K. Sumiyama, H. Ezawa and Y. Nakamura, Phys. Sta. Sol.(a), 93(1986)81.
9) M. Nose and T. masumoto, Sci. Rep. Inst. Tohoku Univ., A-28(1980)232.
P. G. Zielinski, J. Ostatek, M. Kijiek and H.
10) Matyja, Proc. 3rd inst. Conf. Rapidly Quenched metals, vol. 1(1978)p337.